Dynamics of discrete-time quantum walk with time-correlated unitary noise

Y. F. Peng,[1] and X. X. Yi[1,2,*]
[1] *Center for Quantum Sciences and School of Physics, Northeast Normal University, Changchun 130024, China*
[2] *Center for Advanced Optoelectronic Functional Materials Research, and Key Laboratory for UV Light-Emitting Materials and Technology of Ministry of Education, Northeast Normal University, Changchun 130024, China*
(Dated: May 25, 2022)

We investigate the dynamics of discrete-time quantum walk subject to time-correlated noise. Noise is described as an unitary coin-type operator before each step, and attention is focused on the noise generated by a Gaussian Ornstein-Uhlenbeck process, going beyond the usual telegraph noise, where the random variables are consist of only 1 and -1. Under the first-order approximation of BCH formula, the master equation of noisy discrete-time quantum walk is derived. The dynamics given by the master equation are in good agreement with those given by numerical simulations within a certain period of steps, which is controlled by noise parameters. Two remarker behaviors of long time noisy dynamics are observed in numerical simulations, corresponding to two opposite noise regimes: in slow noise regime, with the increase of the noise amplitude, the quantum coherence is suppressed, and the dynamics of noisy discrete-time quantum walk gradually transits to that of classical random walk. In fast noise regime, the walker is confined into few lattice sites, and the width of wave packet is much narrower compared with that in slow noise regime.

PACS numbers:

I. INTRODUCTION

Quantum walk (QW), a natural and straightforward generalization of classical random walk to quantum world, is nowadays a topic of great interest to both theorists and experimentalists [1–3]. Compared with classical random walk (CRW), where information propagates at a speed $\sqrt{t}$, one of those crucial features that QW possess is a much faster expansion of walker proportional to t in position space due to quantum coherence. At certain computational tasks, quantum walks provide exponential speedup over classical computation and are used as a powerful tool in most of efficient quantum algorithms [4–6]. Moreover, with the ability to engineer and control the dynamics of QW by controlling various parameters in evolution operators, QW can also be used to model a wide variety of physical process including photosynthesis [7–9], quantum diffusion [10], optical or spin pumping and vortex transport [11, 12], electrical breakdown [13], localization[14, 15], topological phase [16–21], and so on. Motivated by the prospect of such an array of applications, QW are implemented in numerous experimental setups including quantum optical lattices [22, 23], ion traps [24–26], photons [27–29], and nuclear magnetic resonance [30, 31]. These systems offer the possibility to study quantum dynamics of single or many particles in a precisely controlled experimental setting.

Categorized into two classes, the dynamics of the walker is determined completely by an unitary time evolution. In continuous-time quantum walk [32], the dynamics is described by a Hamiltonian, which defines a progress on continuous time and discrete space, without coin-like degrees of freedom. In discrete-time quantum walk (DTQW) [33], its dynamics is generally implemented by combining conditional shift operators and coin operators, which act on the position of a walker and its associated coin, respectively, evolve in position space involving interference of amplitudes of multiple traversing paths [34–37].

Given their relevance in applications, a realistic description of the dynamics of a quantum walker should take into account disorder induced by noise and imperfections. Lattices dynamics of disordered continuous-time quantum walk has been studied for years, presenting today a well-established theoretical framework. The main characteristic is the localization effect, where studies about the role played by system dimensionality [38], correlations [39], and electron-electron interaction [40]. Different variations of the standard DTQW have also been proposed, such as two entangled particles [41], entangled coins [42], multi-states [43, 44], and alternation of different quantum coins in a certain sequence [45]. For a dynamic disorder, the quantum coins are identical for all lattice sites but change for every step or several steps [46–48]. In this context, the analysis of the time evolution of a quantum walker in the presence of unitary noise in the Hadamard walk show that the standard deviation of the spatial distribution acquires a diffusive behavior for long steps, like the classical random walk.

However, so far, these studies of noisy DTQW are mainly focused on the influence of uncorrelated or space-correlated noise on dynamics. How about the dynamics of DTQW subject to time-correlated noise? Moreover, since noise is introduced to model the interaction between the system and environment, the dynamics averaged over noise realizations should be equivalent to a master equa-

*yixx@nenu.edu.cn

tion. Then, the second question naturally arises: what is the master equation for noisy walking?

The paper is structured as follows: In Sec. II, we introduce the model for a DTQW subject to time-correlated noise. In Sec. III, we derive the master equation of the noisy DTQW and discuss the influence of noise parameters on the valid time of master equation. In Sec. IV, numerical simulations of noisy dynamics are explored. Sec. V closes the paper with some concluding remarks.

II. THE NOISY SPLIT-STEP QUANTUM WALK

Let us begin by considering a protocol, split-step quantum walk (SSQW), which act on a single spin-1/2 particle ($|\uparrow\rangle, |\downarrow\rangle$) in a one dimensional lattice ($|x\rangle, x \in Z$). Parametrized by angles θ_1 and θ_2, a single evolution operator for SSQW is defined by

$$\hat{U}_s = T_\downarrow R_y(\theta_2) T_\uparrow R_y(\theta_1). \tag{1}$$

This protocol consists of a sequence of unitary operations

$$\begin{aligned} R_y(\theta) =& \sum_x e^{-i\theta\sigma_y/2} \otimes |x\rangle\langle x|, \\ T_\uparrow =& \sum_x |x+1\rangle\langle x| \otimes |\uparrow\rangle\langle\uparrow| + |x\rangle\langle x| \otimes |\downarrow\rangle\langle\downarrow|, \\ T_\downarrow =& \sum_x |x\rangle\langle x| \otimes |\uparrow\rangle\langle\uparrow| + |x-1\rangle\langle x| \otimes |\downarrow\rangle\langle\downarrow|. \end{aligned} \tag{2}$$

SSQW, like other quantum systems, inevitably interacts with the environment. This interaction can be described by a variety of noise models. Here, we introduce an unitary noise operator expressed as [46, 49, 50]

$$\hat{U} = \hat{U}_s e^{-i\hat{A}(t)}, \tag{3}$$

where $\hat{U}_s$ is the time evolution operator of the noiseless SSQW and $\hat{A}(t)$ is a Hermitian operator determined by environment. It can be expanded in the bases of Pauli operators such that

$$\hat{A}(t) = \lambda_x(t)\sigma_x + \lambda_y(t)\sigma_y + \lambda_z(t)\sigma_z, \tag{4}$$

where $\lambda_\nu(t), \nu = x, y, z$ are real stochastic variables and $\sigma_{x,y,z}$ are Pauli operators. The dynamics of the walker is computed as the ensemble average [51, 52]

$$\rho(t) = \left\langle \hat{U}(t)\rho(0)\hat{U}^\dagger(t) \right\rangle, \tag{5}$$

where $\rho(0)$ is the initial density matrix and $\langle ... \rangle$ denotes the average of unitary dynamics over all possible realizations of the stochastic processes. Here, for simplicity, we assume that $\lambda_\nu(t) = \gamma_\nu \zeta_\nu(t)$. $\zeta_\nu(t)$ comes from Gaussian process satisfying

$$\begin{aligned} \langle \zeta_\nu(t) \rangle =& 0, \\ \langle \zeta_\nu(t)\zeta_{\nu'}(t') \rangle =& \delta_{\nu,\nu'} K(t,t'). \end{aligned} \tag{6}$$

Although DTQW can be implemented by linear optical components as in [53], this increases the experimental complexity in terms of optical stability, alignment, and cost. Based on [27], we present a scheme to implement the noisy SSQW on a optical feedback loop as illustrated in Fig. 1. In this scheme, different path lengths in the circuit generate temporally encoded states, where different position states are represented by discrete time bins. The stochastic unitary operation $e^{-i\hat{A}(t)}$ is implemented by two electro-optic modulators (EOM) that always maintain the same input electric field to output the same stochastic signals. Two coin operations $R_y(\theta_1)$ and $R_y(\theta_2)$ are implemented by half-wave plate (HWP) H_1 and H_2, separately. The photonic wave packets are split by a polarizing beam splitter(PBS) P_1 and routed through single-mode fibers(SMF) of different length, which are labeled by $x+1$ and x, respectively. Considering the packet x arrives P_2 firstly, therefore, in chronological order, wave packets are $x-1$, x and x, $x+1$ are detected successively. Then, some photons are reflected by a beam splitter(BS) for detection and the transmitted photons continue to go through the circuit.

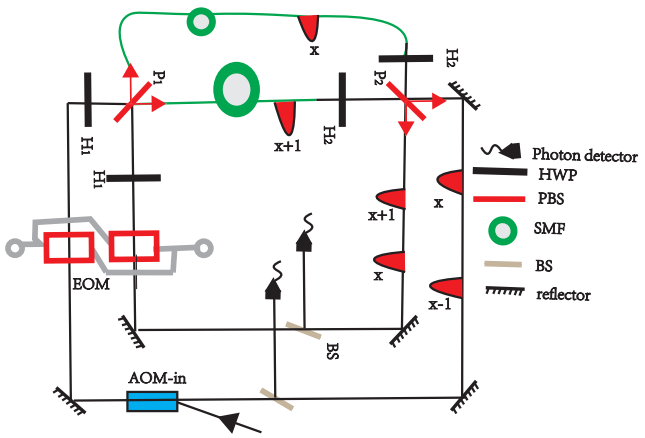

FIG. 1: Sketch of the setup. The initial pulse is generated from an pulsed laser, and is coupled into the circuit by an acousto-optic modulator (AOM). H_1 and H_2 represent the rotation operations $R_y(\theta_1)$ and $R_y(\theta_2)$, respectively. P_1 and P_2, implement the step operations T_1 and T_2, respectively. The gray circles of EOM represents the input and output of external voltage, respectively. Two green circles represent two SMF with different lengths to produce temporally encoded states.

III. MASTER EQUATION OF NOISY SSQW

The effects of noise in coin operator or conditional translation on the behaviors of a DTQW have been extensively studied [46, 48, 54]. These studies have pointed that the dynamics of noisy DTQW averaged over all possible realizations equals to that of a walker interacting with environment, however, expression for the master

equation is still unknown. Faced with this problem, we derive a master equation in this article. The reduced dynamics of a system embedded in an environment is generally described by a master equation of this form

$$\frac{d}{dt}\rho(t) = -\frac{i}{\hbar}\left[\hat{H}_s, \rho(t)\right] + \mathcal{D}\left[\rho(t)\right], \tag{7}$$

where $\rho(t)$ is the reduced density matrix of a walker, with Hamiltonian $\hat{H}_s$, interacting with an environment. The first term on the right-hand side accounts for the unitary part of the evolution; The second term accounts for the nonunitary dynamics resulting from the interaction with the environment. In this picture, decoherence is simulated by averaging over an ensemble of these stochastic but unitary quantum dynamics. Although the step protocol is defined explicitly in terms of the discrete unitary operations $T_{\uparrow,\downarrow}$ and $R_y(\theta)$, the net evolution over one step is equivalent to that generated by a time-independent effective Hamiltonian over the step time , i.e., $e^{-i\hat{H}_s} = \hat{U}_s$. Based the translational symmetry of this protocol, in the quasimomentum basis $|k\rangle = (1/\sqrt{N})\sum_k e^{-ikx}|x\rangle$, where N is the number of lattice sites, the effective Hamiltonian $\hat{H}_s$ can be expressed as

$$\hat{H}_s = \sum_k \left[E(k)\vec{n}(k))\cdot\vec{\sigma}\right] \otimes |k\rangle\langle k|. \tag{8}$$

The energy and the components of the Bloch vector are given by

$$\begin{aligned}\cos E(k) = &\cos(\theta_1/2)\cos(\theta_2/2)\cos k \\ &- \sin(\theta_1/2)\sin(\theta_2/2),\end{aligned} \tag{9}$$

and $\vec{n}(k) = n_x(k)\vec{i} + n_y(k)\vec{j} + n_z(k)\vec{k}$ with

$$\begin{aligned}n_x(k) &= \frac{\sin(\theta_1/2)\cos(\theta_2/2)\sin k}{\sin E(k)}, \\ n_y(k) &= \frac{\cos(\theta_1/2)\sin(\theta_2/2) + \sin(\theta_1/2)\cos(\theta_2/2)\cos k}{\sin E(k)}, \\ n_z(k) &= \frac{-\cos(\theta_1/2)\cos(\theta_2/2)\sin k}{\sin E(k)}.\end{aligned} \tag{10}$$

$\hat{U} = e^{-i\hat{H}_s}e^{-i\hat{A}(t)} = e^{-i\hat{H}(t)}$, up to the first-order commutation relation of BCH formula, this approximate expression for $\hat{H}(t)$ is written as:

$$\hat{H}_{st}(t) = \hat{H}_s + \sum_\nu \lambda_\nu(t)\hat{L}_\nu, \tag{11}$$

where $\nu = x, y, z$ with

$$\begin{aligned}\hat{L}_x &= \sum_k \left(\sigma_x + \lambda_k(\vec{n}\times\vec{\sigma})_x\right)\otimes|k\rangle\langle k|, \\ \hat{L}_y &= \sum_k \left(\sigma_y + \lambda_k(\vec{n}\times\vec{\sigma})_y\right)\otimes|k\rangle\langle k|, \\ \hat{L}_z &= \sum_k \left(\sigma_z + \lambda_k(\vec{n}\times\vec{\sigma})_z\right)\otimes|k\rangle\langle k|.\end{aligned} \tag{12}$$

The Hamiltonian of the quantum simulator, $\hat{H}_{st}(t)$, is composed of the target Hamiltonian, $\hat{H}_s(t)$, describing the system one aims at simulating, and a stochastic part that includes a set of Hermitian operators $\hat{L}_\nu$ with noisy coupling $\lambda_\nu(t)$. This stochastic part will be used to engineer the dissipator in Eq. (7).

The stochastic density matrix corresponding to one realization of the Gaussian processes, $\rho_{st}(t) = |\psi_{\rm st}(t)\rangle\langle\psi_{\rm st}(t)|$, is given in terms of the pure state $|\psi_{\rm st}(t)\rangle$, which is obtained from the exact solution of the Schrödinger equation generated by the stochastic Hamiltonian implemented in the simulator, $\hat{H}_{st}(t)$ in Eq. (11). Its time evolution is described by the stochastic Liouville equation

$$\frac{d}{dt}\rho_{st}(t) = -i\left[\hat{H}_s, \rho_{st}(t)\right] - i\sum_\nu \gamma_\nu\left[\zeta_\nu(t)\hat{L}_\nu, \rho_{st}(t)\right]. \tag{13}$$

Averaging over different realizations of stochastic processes $\zeta_\nu(t)$, we obtain the dynamics for the noise averaged density matrix

$$\frac{d}{dt}\langle\rho_{st}(t)\rangle = -i\left[\hat{H}_s, \langle\rho_{st}(t)\rangle\right] + \mathcal{D}[\rho_{st}(t)], \tag{14}$$

where $\mathcal{D}[\rho_{st}(t)] = -i\sum_\nu \gamma_\nu\left[\hat{L}_\nu, \langle\zeta_\nu(t)\rho_{st}(t)\rangle\right]$. Comparing Eq. (14) with Eq. (7), the master equation describing the reduced dynamics of a open systems, enables us to identify the second term on the right-hand side as a dissipator responsible for an effective nonunitary evolution of the noise-averaged density matrix. Since the stochastic density matrix is a functional of the stochastic field $\zeta_\nu(t)$, the explicit form of the dissipator can be derived by using Novikov's theorem [51, 55], which gives the mean value of a product of a Gaussian noise with its functional

$$\langle\zeta_\nu(t)\rho_{st}\left[\zeta_\nu(t)\right]\rangle = \int_0^t \langle\zeta_\nu(t)\zeta_\nu(t')\rangle\left\langle\frac{\delta\rho_{st}\left[\zeta_\nu(t)\right]}{\delta\zeta_\nu(t')}\right\rangle dt'. \tag{15}$$

The functional derivative can be obtained from the stochastic density matrix $\rho_{st}(t) = \hat{U}_{st}(t,t')\rho_{st}(t')\hat{U}_{st}^\dagger(t,t')$, where time evolution operator $\hat{U}_{\rm st}(t,t') = \mathcal{T}\exp\left[-i\int_{t'}^t \hat{H}_{st}(s)ds\right]$ and $\mathcal{T}$ denotes the time-ordering operator. Therefore, partial differentiation reads:

$$\frac{\delta\rho_{st}(t)}{\delta\zeta_\nu(t')} = U_{st}(t,t')\left(-i\gamma_\nu\left[\hat{L}_\nu, \rho_{st}(t')\right]\right)U_{st}^\dagger(t,t'). \tag{16}$$

Using this expression, the master equation for the noise-averaged density matrix is derived as:

$$\begin{aligned}\frac{d}{dt}\langle\rho_{st}(t)\rangle = &-i\left[\hat{H}_s, \langle\rho_{st}(t)\rangle\right] - \sum_\nu \gamma_\nu^2\int_0^t dt' K(t,t') \\ &\times\left[\hat{L}_\nu, \left\langle\left[\hat{U}_{st}(t,t')\hat{L}_\nu\hat{U}_{st}(t,t'), \rho_{st}(t)\right]\right\rangle\right].\end{aligned} \tag{17}$$

In this part, the initial state $|\psi(0)\rangle = |x_0\rangle \otimes (1/\sqrt{2}(|\uparrow\rangle - i\,|\downarrow\rangle)$ with $N = 141$ and $\theta_1 = 0.2\pi, \theta_2 = 0.3\pi$. Here we consider time-correlated Ornstein-Uhlenbeck process

$$\langle \zeta_{\rm i}(t_1)\zeta_j(t_2)\rangle = \delta_{ij}\gamma^2 e^{-(t_1-t_2)/\tau}. \tag{18}$$

We are interested in the dynamics under different amplitudes as its correlation time is tuned from the Markovian, white noise limit, $\tau \to 0$, to the limit of the quasi-static noise, $\tau \to \infty$. The selected parameters can well reflect the dynamic changes of the system when the transition from Markovian noise to quasi-static noise. We compare the distribution of the analytical results obtained by Eq. (17) with those of the numerical results obtained by Eq. (5) via the similarity $S = \left[\sum_x \sqrt{P_a(t)P_n(t)}\right]^2$ [27], quantifying the equality of two probability distributions ($S = 0$ for completely orthogonal distributions and $S = 1$ for identical distributions). Here, we make an appointment that only $S > 0.72$, the analytical results can describe the noisy dynamics well.

Markovian case.— The form of the dissipator greatly simplifies when the stochastic variables $\{\zeta_\nu(t)\}$ are described by independent white noises such that $K(t,t') = \delta(t-t')$. In particular, the dissipator now only depends on the average density operator $\langle\rho_{st}(t)\rangle$, that we hereafter denote by $\rho(t)$ to simplify the notation. Eq. (17) reduces in this case to

$$\frac{d}{dt}\rho(t) = -i\left[\hat{H}_s, \rho(t)\right] - \sum_\nu \gamma_\nu^2 \left[\hat{L}_\nu, \left[\hat{L}_\nu, \rho(t)\right]\right]. \tag{19}$$

The dynamics are shown in Fig. 2.

Generalization to non-Markovian dynamics.— While the use of white noise leads to a Lindblad dissipator simulating Markovian dynamics, a non-Markovian evolution can be obtained using colored noise. To second order in the strength of the noise, after approximating $\hat{U}_{st}(t,t')$ by $\hat{U}_{\rm s}(t,t') \equiv e^{-iH_s(t-t')}$, the master equation for colored noise is derived as follows

$$\frac{d}{dt}\rho(t) = -i\left[\hat{H}_s, \rho(t)\right] - \sum_\nu \gamma_\nu^2 \int_0^t dt' e^{(t-t')/\tau}\left[\hat{L}_\nu, \left[\hat{L}_\nu(t,t'), \rho(t)\right]\right], \tag{20}$$

where $\hat{L}_\nu(t,t') = \hat{U}_{\rm s}(t,t')\hat{L}_\nu\hat{U}_s^\dagger(t,t')$. The probability distribution are shown in Fig. 3.

Each white-dashed line in Fig. 2 and Fig. 3 means that only before this evolution step, the similarity between analytical result and numerical result is greater than the agreed value (0.72), the master equation derived from Eq. (11) can well describe the noisy walk, therefore, it is valid during this period. In fact, $e^{-i\hat{H}_s}e^{-i\hat{A}(t)} = e^{-i\hat{H}(t)} = e^{-i\hat{H}_{st}(t)-i\hat{H}_e(t)}$, however, to get the Hamiltonian in Eq. (11), we ignore $\hat{H}_e$, which can be written as polynomials of noise parameters like $\sum_n \gamma^n \hat{P}_n$ with $n > 1$. Therefore, with the increase of evolution steps, the impact of this part on the dynamics gradually appears, and the similarity of the two results naturally decreases. The larger the noise amplitude, the greater the influence of this part on dynamics, so the valid time of master equation is shorter under the same correlation time. This is well reflected in Fig. 2 and Fig. 3. Moreover, the results show that steps for the similarity decreasing to the agreed value (0.72) for $\tau = 0.1, \gamma = 0.3$ is shorter than that for $\tau = 10, \gamma = 1$. Noise sequence with longer correlation time is smoother than that with short correlation time, and noisy SSQW with a smooth sequence means that the difference between the stochastic noise operators of two consecutive steps is small. So, the impact of noise on dynamic is weaker for $\tau = 10, \gamma = 1$ compared with that for $\tau = 0.1, \gamma = 0.3$, and we can even infer that with the same noise amplitude, a longer correlation time induces a longer valid time of the master equation.

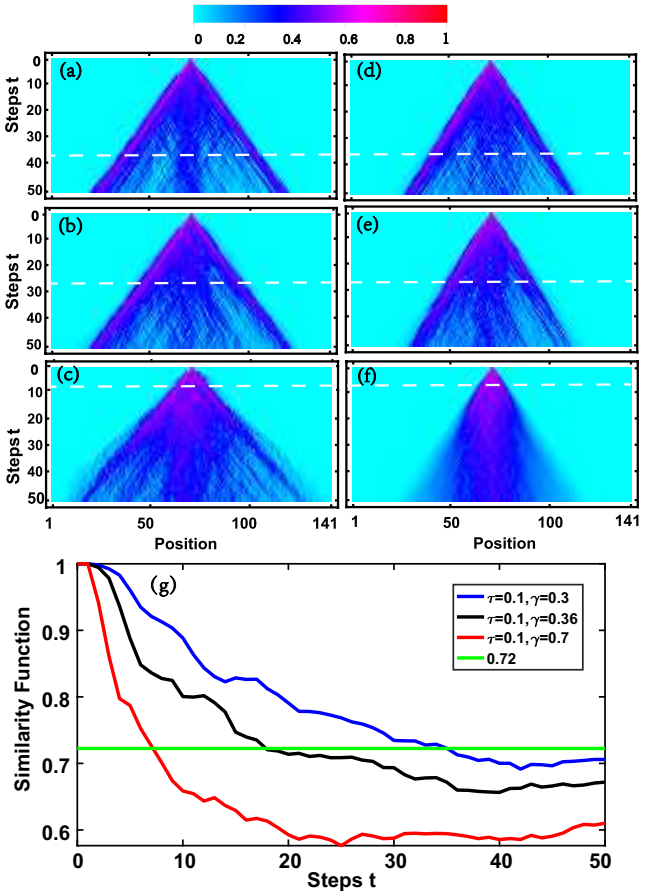

FIG. 2: Time evolution of the density of probability in position space of a quantum walker on chains. (a)-(c) are analytical results for $\tau = 0.1$, $\gamma = 0.3, 0.36, 0.7$, and (d)-(f) are numerical results for $\tau = 0.1$, $\gamma = 0.3, 0.36, 0.7$, respectively. (g) is the function of similarity to time. The steps t specified by white dotted lines in (a)-(f) are horizontal ordinates of the intersection point of the green line and the similarity function for $\gamma = 0.3, 0.36, 0.7$.

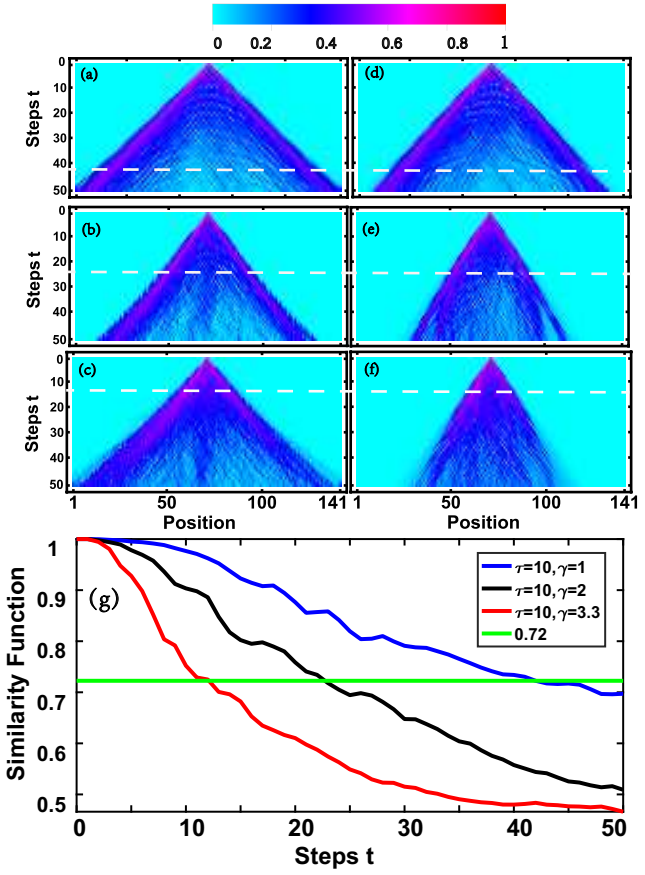

FIG. 3: Time evolution of probability in position space of a quantum walker on chains. (a)-(c) are analytical results for $\tau = 10$, $\gamma = 1, 2, 3.3$, and (d)-(f) are numerical results for $\tau = 10$, $\gamma = 1, 2, 3.3$, respectively. (g) is the function of similarity to time. The steps t specified by the white-dashed lines in (a)-(f) are horizontal ordinates of the intersection point of the green line and the similarity function for $\gamma = 1, 2, 3.3$, respectively.

IV. NUMERICAL SIMULATIONS OF NOISY DYNAMICS

Since the master equation can describe the noisy dynamics well within a certain steps t, which is affected by noise parameters. To explore long-time behavior of noisy SSQW, numerical simulations with representative noise parameters are necessary. Under the action of Ornstein-Uhlenbeck process, the walker spreads over the lattice with a probability distribution relevant to the amplitude γ and correlation time τ. The correlation function of Ornstein-Uhlenbeck process is similar to that of telegraph noise studied in [39], so, $\tau = 0.1$ and $\tau = 10$ are chosen as representative parameters for fast noise and slow noise in this work, respectively. Besides, in Eq. (11), $\sum_\nu \lambda_\nu(t) L_\nu$ can be seen as $\hat{H}_A + \hat{H}_{A,s}$, where $\hat{H}_A$ is the Hamiltonian of noise and $\hat{H}_{A,s}$ can be seen as the interaction Hamiltonian. Since this part role as a perturbation, one can require the energy of this part, E_p, does not exceed E_s, the energy of $\hat{H}_s$, ie, $|\langle E_p \rangle| \leq |E_S| \leq \pi$. $|\langle E_p \rangle| \geq |\langle E_A \rangle| = \sqrt{3}\gamma$, therefore, noise amplitude γ should be limited between 0 and $\sqrt{\pi^2/3}$. In practice, in order to make the noisy dynamics more distinguishable, we consider $\gamma \in [0, 4]$. Moreover, we have numerically test the dynamics for all kinds of noise parameters, the probability distribution of each sites may be different, but, the shapes of the distributions are included in the results we have discussed. So, the present results are sufficient for the study of noisy dynamics.

Each column in Fig. 4 shows the probability distribution of the walker over lattice sites at three different evolution steps with representative noise parameters. From (a)-(c), one observes that when $\tau = 10$ (slow decaying autocorrelation function), noise amplitude $\gamma = 0.1$, the final state clearly shows the characteristic shape of an unperturbed SSQW: the two pronounced side peaks and the low probability around the initial position; While, two tail peaks are suppressed, the central part grows and a Gaussian-type distribution centered around the initial position arise as the noise amplitude γ is increased, which means a transition from quantum to classical. In (d)-(f), $\tau = 0.1$, noise is chosen from a stochastic process with fast decaying autocorrelation function. when $\gamma = 0.1$, the effects of the competition between the behavior of noiseless SSQW and unitary noise are clearly shown. First, oscillating wings on the edges, an incoherent component is generated around the center. Gradually, the central peak increases absorbing weight from the two oscillating wings, which later disappear completely. As for the probability distribution $P_t(x)$ for $\tau = 0.1, \gamma = 0.8$, at this noise level, the quantum effects are completely suppressed by the noise in several steps, and then the oscillations are smoothed and converges towards a Gaussian distribution in few lattice sites, which expands with time. The outlines for the probability distribution with $\tau = 0.1, \gamma \geq 0.8$ are almost identical. Besides, by comparing the dynamics with the same noise amplitudes and different correlation times, one can also find that long noise correlation time is helpful to reduce the damage of noise to quantum coherence. What emerges from our analysis, so far, is that in time-correlated noise regime, we see a transition from quantum to classical diffusive behavior. The influence of noise on dynamics of the walker may be analyzed in more details by looking at the time dependency of the averaged standard deviation $\langle \sigma(t) \rangle = \left\langle \sqrt{\sum_x x^2 P_t(x) - (\sum_x x P_t(x))^2} \right\rangle$ of the spacial distribution. As we know, transport properties of DTQW are quite different from those of CRW, which mainly originate from the principle of superposition of quantum mechanics. For noiseless SSQW, probability distribution of the walker exhibits a ballistic behavior, and the standard deviation $\sigma(t) = q_0 t$, where $q_0 \approx 0.45$ and $\sigma = \sqrt{t}$ for the classical random walk [46]. For $\tau = 10$, $\gamma = 0.1$, a weak noise with slow decaying correlation function, the averaged standard derivation can be expressed as $\langle \sigma(t) \rangle = qt$ with $q = 0.42$, which is very close to the q_0. This value also corresponds to the high similarity between the prob-

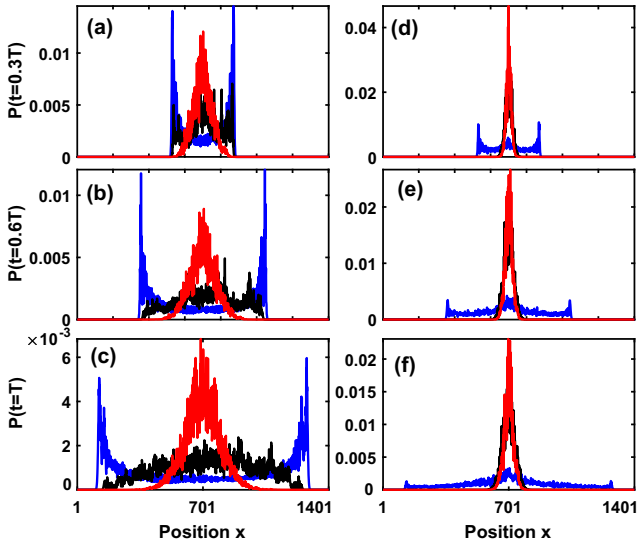

FIG. 4: Probability distribution of a walker over the lattices. From here, the particle is initially at the localized state $|1+(N-1)/2\rangle \otimes (|\uparrow\rangle - i\,|\downarrow\rangle)/\sqrt{2}$ with $N = 1401$, $\theta_1 = 0.2\pi$ and $\theta_2 = 0.3\pi$. The total evolutionary steps is $T = 1000$; The noise correlation time τ for (a)-(c) and (d)-(f) are 10 and 0.1, respectively. And the blue, black and red lines represent noise amplitudes $\gamma = 0.1, 0.8, 4$, respectively.

ability distribution for this parameter and that for noiseless walking. These results show that the standard deviation curves for noisy SSQW move down from the top curve of an almost noiseless quantum walk to the bottom curve describing the classical random walk as the noise level increases or noise correlation time decreases. Besides, for the dynamics with the same noise amplitude, the longer the correlation time is, the more sites the wave function reaches, and therefore the larger the standard derivation is.

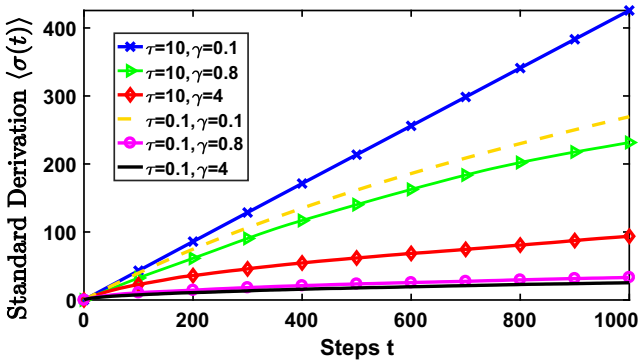

FIG. 5: The averaged standard deviation $\langle\sigma(t)\rangle$ as a function of evolution steps for SSQW subject to Ornstein-Uhlenbeck process with different noise parameters.

So far, the dynamic characteristics of SSQW subject to time correlated noise have been explored, now, we focus our attention on its genuine quantum features. Unitary coin operation $R_y(\theta)$ acting only on the walker's internal degree of freedom, leaving it generally in a superposition of spin up and spin down. Conditional translation $T_{\uparrow,\downarrow}$ relate the displacement of the walker to its internal degree of freedom. In this way, spin and position of the system are entangled, and the evolution of SSQW creates a superposition among the position states of the system, opening the way for interference effects to take place that ultimately determine the ballistic behavior for the displacement of the quantum walker. Entanglement and interference are genuine quantum features of DTQW since there are no analogs for CRW[56, 57].

The total initial state (spin plus position) $|\psi(0)\rangle$ is always pure in this paper. This, together with the fact that the evolution of the whole system is unitary, leads to total pure states at any time. In this scenario, the natural choice to quantify the entanglement between the internal and external degrees of freedom is the von Neumann entropy S_E of the partially reduced state of either the spin or position, with either choice furnishing the same entanglement [58]. The simplest choice is to work with the spin-reduced state

$$S_E(t) = -Tr[\rho_c(t)\log_2\rho_c(t)] \tag{21}$$

where $\rho_c(t) = Tr_p[\rho(t)]$, $\rho(t) = |\psi(t)\rangle\langle\psi(t)|$ and $Tr_p(.)$ is the trace over position degrees of freedom. As can be seen from Fig. 6, the average entanglements $\langle S_E(t)\rangle$ of noisy SSQW approach the maximal value possible $S_E = 1$ for fast and slow noise. Increasing the noise amplitude or shortening the correlation time, it evolves to the asymptotic values 1 more quickly. Therefore, dynamically disordered SSQW can be used as a maximal entanglement generator, outperforming the entanglement attained by using ordered SSQW. Since $\rho_c(t) = \alpha(t)\,|\uparrow\rangle\langle\uparrow| + \beta(t)\,|\downarrow\rangle\langle\downarrow| + \gamma(t)\,|\uparrow\rangle\langle\downarrow| + \gamma^*(t)\,|\downarrow\rangle\langle\uparrow|$, $S_E(t) = -\lambda_+(t)\log_2\lambda_+(t) - \lambda_-(t)\log_2\lambda_-(t)$, with $\lambda_\pm = 1/2 \pm \sqrt{1/4 - \alpha(t)\,[1-\alpha(t)] + |\gamma(t)|^2}$, we numerically prove the asymptotic behavior of the average entanglement $\langle S_E(t)\rangle$. In Fig. 7 (a)-(d), $\gamma(t)$ and $|\alpha(t)|$ will eventually saturate to 0 and 1/2, respectively, which mean that $\rho_c(t) = \rho_c(t+1) = 1/2\,|\uparrow\rangle\langle\uparrow| + 1/2\,|\downarrow\rangle\langle\downarrow|$ for $t \to \infty$, therefore, that $\langle S_E(t)\rangle$ for different noise parameters evolves to the asymptotic values 1 is reasonable. However, the steps needed to reach the saturation value depend on the noise parameters. $\alpha(t)$ are stable around 0.5, so $\langle S_E(t)\rangle$ mainly depends on the root part of $\lambda_\pm$. Shortening the correlation time or increasing the noise amplitude can accelerate the time for $\gamma(t)$ to saturation value 0, so the asymptotic time of the entanglement entropy is controlled.

Quantum coherence makes QW different from the classical random walk, and the analysis of the probability distribution over lattice sites and the standard derivation only involve the diagonal elements of the density matrix. In order to gain more insight into the behavior of the system, we study its coherence C. The coherence of a quantum state is investigated by adopting the nor-

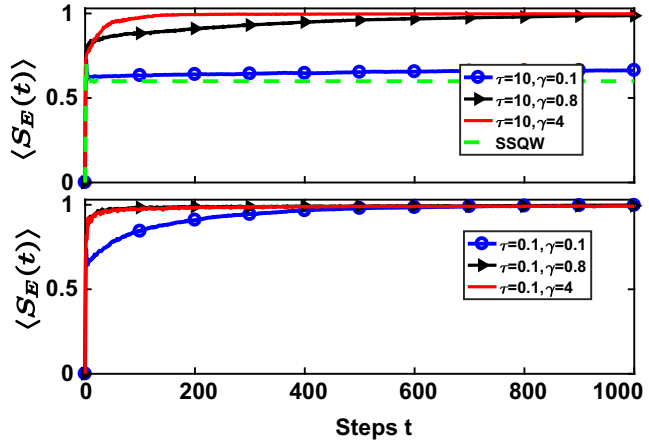

FIG. 6: The averaged entanglement entropy $\langle S_E(t)\rangle$ as a function of time for SSQW subject to Ornstein-Uhlenbeck process with different noise parameters.

malized coherence measure proposed in [59, 60]:

$$C(t) = \frac{1}{N-1}\sum\nolimits_{i\neq j} |\widetilde{\rho}_{ij}(t)|, \tag{22}$$

where N is the dimensionality of position Hilbert space and $\widetilde{\rho}$ is obtained by taking trace of $\rho(t)$ over spin degrees of freedom. Fig. 8 shows the coherence for noisy SSQW for representative noise parameters. In slow noise regime, the off-diagonal elements of the reduced density matrix grow over time, and the larger the noise amplitude γ, the smaller the increment of coherence during same evolution steps. In fast noise regime, the coherence $\langle C(t)\rangle$ for $\tau = 0.1, \gamma = 0.1$ increases over steps, but that for $\tau = 0.1, \gamma = 0.8$ and $\tau = 0.1, \gamma = 4$ increase quite slowly, which indicates the survival of quantumness over time, as expected the Anderson localization in the dynamical counterpart. We also noticed that the behaviors of $\langle C(t)\rangle$ with different noise parameters are similar to the standard derivation $\langle\sigma(t)\rangle$ in Fig. 5. In fact, their similar behaviors are natural. Coherence describes the wave nature, the bigger the coherence, the more sites the wave packet reaches, and therefore, the larger the standard deviation $\langle\sigma(t)\rangle$.

V. SUMMARY

We have studied the dynamics of SSQW subject to unitary noise. Noise have been modeled as stochastic unitary coin before each step to reflect the change of spin state exposed to a random environment. The dynamics of a walker has been computed as an ensemble average over possible realizations of the noise. We found that the dynamics obviously depends on two parameters of noise: correlation time and amplitude. Correlation time reflects the similarity of stochastic process computed by correlation function, and noise amplitude reflects the coupling between the system and environment. In fast noise regime, i.e., similarity of a stochastic process decreases rapidly over time, noise sequence is rough, the walker undergoes time disordered unitary evolutions and is finally confined into few lattice sites under strong noise amplitude. In slow noise regime, the final state of a weakly coupled walker clearly shows the characteristic shape of an noiseless SSQW, and a transition from quantum ballistic diffusion to classical diffusive propagation over lattice sites as the noise amplitude γ is increased. The transition behavior is also observed in the standard derivation. Entanglement, as a genuine quantum features of noisy SSQW, approaches the maximum possible value ($\langle S_E(t)\rangle = 1$) eventually and the evolution steps to reach the asymptotic value depends on the noise parameters. Shortening the correlation time or enhancing the noise amplitude can accelerate this process. Coherence, the other quantum feature, its behavior is similar to that of the stand derivation, and this result stresses that coherence makes quantum walk different from classical random walk.

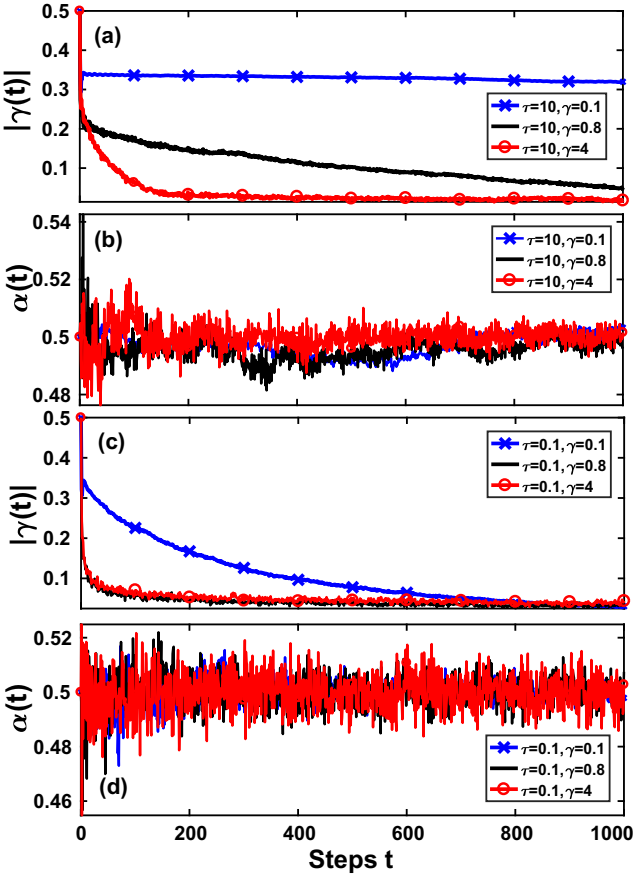

FIG. 7: Matrix elements of $\rho_c(t)$ as functions of steps t for different noise parameters. Noise amplitude in (a)-(d) are set as $\gamma = 0.1$ (blue crossed lines), $\gamma = 0.8$ (black lines) and $\gamma = 4$ (red circled lines), and correlation times are chosen to represent slow ($\tau = 10$) regime in (a)-(b) and fast ($\tau = 0.1$) regime in (c)-(d).

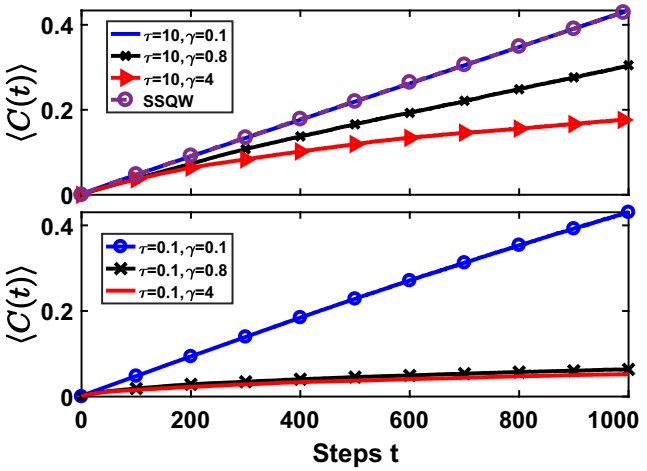

FIG. 8: The averaged coherence $\langle C(t)\rangle$ as a function of steps t for noisy SSQW with different noise parameters.

VI. ACKNOWLEDGMENTS

Thanks my colleagues for helpful discussions and Jinlei Li for shearing the technical details used in the calculation. This work is supported by National Natural Science Foundation of China (NSFC) under Grants No. 11775048, and No.11947405.

[1] Y. Aharonov, L. Davidovich, and N. Zagury, "Quantum random walks," Phys. Rev. A **48**, 1687 (1993).
[2] E. Farhi and S. Gutmann, "Quantum computation and decision trees," Phys. Rev. A **58**, 915 (1998).
[3] J. Kempe, "Quantum random walks: An introductory overview," Comtemp. Phys. **44**, 307 (2003).
[4] E. Farhi and S. Gutmann, "Quantum computation and decision trees," Phys. Rev. A **58**, 915 (1998).
[5] A. M. Childs and J. Goldstone, " Spatial search by quantum walk," Phys. Rev. A **70**, 022314 (2004).
[6] A. M. Childs, " Universal Computation by Quantum Walk," Phys. Rev. Lett. **102**, 180501 (2009).
[7] R. J. Sension, " Quantum path to photosynthesis," Nature(London) **446**, 740-741 (2007).
[8] G. S. Engel, T. R. Calhoun, E. L. Read, T. K. Ahn, T. Manal, Y. C. Cheng, R. E. Blankenship, and G. R. Fleming, " Evidence for wavelike energy transfer through quantum coherence in photosynthetic systems," Nature(London) **446**, 782C786 (2007).
[9] M. Mohseni, P. Rebentrost, S. Lloyd, and A. Aspuru-Guzik, " Environment assisted quantum walks in photosynthetic energy transfer," J. Chen. Phys. **129**, 174106 (2008).
[10] S. Godoy and S. Fujita, " A quantum random walk model for tunneling diffusion in a 1D lattice. A quantum correction to Ficks law," J. Chen. Phys. **97**, 5148 (1992).
[11] M. S. Rudner and L. S. Levitov, " Topological Transition in a Non-Hermitian Quantum Walk," Phys. Rev. Lett. **102**, 065703 (2009).
[12] S. Hoyer and D. A. Meyer, " Faster transport with a directed quantum walk," Phys. Rev. A **79**, 024307 (2009).
[13] T. Oka, N. Konno, R. Arita, and H. Aoki, " Breakdown of an Electric-Field Driven System: A Mapping to a Quantum Walk," Phys. Rev. Lett. **94**, 100602 (2005).
[14] C. Lyu, Luyan Yu, Shengjun Wu, and M. S. Kim, "Localization in quantum walks on a honeycomb network," Phys. Rev. A **92**, 052305 (2015).
[15] X. P. Xu, Y. Ide, and N. Konno, "Symmetry and localization of quantum walks induced by an extra link in cycles," Phys. Rev. A **85**, 042327 (2012).
[16] J. K. Asbth and H. Obuse, "Bulk-boundary correspondence for chiral symmetric quantum walks," Phys. Rev. B **88** , 121406(R) (2013).
[17] E. Flurin, V. V. Ramasesh, S. H. Gourgy, L. S. Martin, N. Y. Yao, and I. Siddiqi, "Observing Topological Invariants Using Quantum Walks in Superconducting Circuits," Phys. Rev. X **7**, 031023 (2017).
[18] X. P. Wang, L. Xiao, X. Z. Qiu, K. k. Wang, W. Yi, and P. Xue, "Detecting topological invariants and revealing topological phase transitions in discrete-time photonic quantum walks," Phys. Rev. A **98**, 013835 (2018).
[19] X. Zhan, L. Xiao, Z. Bian, K. Wang, X. Qiu, B. C. Sanders, W. Yi, and P. Xue, "Detecting Topological Invariants in Nonunitary Discrete-Time Quantum Walks," Phys. Rev. Lett. **119**, 130501 (2017).
[20] L. Xiao, X. Z. Qiu, K. k. Wang, Z. H. Bian, X. Zhan, H. Obuse, B. C. Sanders, W. Yi, and P. Xue, "Higher winding number in a nonunitary photonic quantum walk," Phys. Rev. A **98**, 063847 (2018).
[21] T. Kitagawa, M. S. Rudner, E. Berg, and E. Demler, "Exploring topological phases with quantum walks," Phys. Rev. A **82**, 033429 (2010).
[22] W. Dr, R. Raussendorf, V. M. Kendon, and H. J. Briegel, "Quantum walks in optical lattices," Phys. Rev. A **66**, 0523197 (2002).
[23] L. M. Wang, L. Wang, and Y. B. Zhang, "Quantum walks of two interacting anyons in one dimensional optical lattices," Phys. Rev. A **90**, 03618 (2014).
[24] H. Schmitz, R. Matjeschk, Ch. Schneider, J. Glueckert, M. Enderlein, T. Huber, and T. Schaetz, "Quantum Walk of a Trapped Ion in Phase Space," Phys. Rev. Lett. **103** , 090504 (2009).
[25] F. Z. hringer, G. Kirchmair, R. Gerritsma, E. Solano, R. Blatt, and C. F. Roos, "Realization of a Quantum Walk with One and Two Trapped Ions," Phys. Rev. Lett. **104**, 100503 (2014).
[26] A. R. C. Buarque and W. S. Dias, "Self-trapped quantum walks ," Phys. Rev. A **101**, 023802 (2020).

[27] A. Schreiber, K. N. Cassemiro, V. Potoček, A. Gabris, P. J. Mosley, E. Andersson, I. Jex, and Ch. Silberhorn, "Photons Walking the Line: A Quantum Walk with Adjustable Coin Operations," Phys. Rev. Lett. **104**, 050502 (2010).

[28] M. A. Broome, A. Fedrizzi, B. P. Lanyon, I. Kassal, A. Aspuru-Guzik, and A. G. White, "Discrete Single-Photon Quantum Walks with Tunable Decoherence," Phys. Rev. Lett. **104**, 153602 (2010).

[29] A. Schreiber, A. Gábris, P. P. Rohde, K. Laiho, M. Štefaňák, V. Potoček, C. Hamilton, I. Jex, and C. Silberhorn, "A 2D Quantum Walk Simulation of Two-Particle Dynamics," Science **336**, 55 (2012).

[30] C. A. Ryan, M. Laforest, J. C. Boileau, and R. Laflamme, " Experimental implementation of a discrete-time quantum random walk on an NMR quantum-information processor," Phys. Rev. A **72** , 062317 (2005).

[31] J. Du, H. Li, X. Xu, M. Shi, J. Wu, X. Zhou, and R. Han, " Experimental implementation of the quantum random-walk algorithm," Phys. Rev. A **67** , 042316 (2003).

[32] L. Wang, N. Liu, S. Chen, and Y. B. Zhang , " Quantum walks accompanied by spin flipping in one-dimensional optical lattices," Phys. Rev. A **92** , 053606 (2015).

[33] S. E. V. Andraca, " Quantum walks: a comprehensive review," Quant. Info. Proc. **11** , 1501-1506 (2012).

[34] P. L. Knight, E. Roldn, and J. E. Sipe, "Quantum walk on the line as an interference phenomenon," Phys. Rev. A **68**, 020301 (2003).

[35] C. M. Chandrashekar, "Disordered-quantum-walk-induced localization of a Bose-Einstein condensate," Phys. Rev. A **83**, 022320 (2011).

[36] H. Jeong, M. Paternostro, and M. S. Kim, "Simulation of quantum random walks using the interference of a classical field," Phys. Rev. A **69**, 012310 (2004).

[37] V. Kendon and B. C. Sanders, "Complementarity and quantum walks," Phys. Rev. A **71**, 022307 (2005).

[38] E. Abrahams, P. W. Anderson, D. C. Licciardello, and T. V. Ramakrishnan, "Scaling Theory of Localization: Absence of Quantum Diffusion in Two Dimensions," Phys. Rev. Lett. **42**, 673 (1979).

[39] C. Benedetti, F. Buscemi, P. Bordone, and M. G. A. Paris, "Non-Markovian continuous-time quantum walks on lattices with dynamical noise," Phys. Rev. A **93**, 042313 (2016).

[40] K. Byczuk, W. Hofstetter, and D. Vollhardt, "Mott-Hubbard Transition versus Anderson Localization in Correlated Electron Systems with Disorder," Phys. Rev. Lett. **94**, 056404 (2005).

[41] I. Siloi, C. Benedetti, E. Piccinini, J. Piilo, S. Maniscalco, M. G. A. Paris, and P. Bordone, "Noisy quantum walks of two indistinguishable interacting particles," Phys. Rev. A **95**, 022106 (2017).

[42] S. E. V. Andraca, J. L. Ball, K. Burnett, and S. Bose, "Quantum walks with entangled coins," New J. Phys. **7**, 221 (2005).

[43] N. Inui and N. Konno, "Localization of multi-state quantum walk in one dimension," Physica A **353**, 133 (2005).

[44] N. Inui, N. Konno, E. Segawa, M. G. A. Paris, and P. Bordone, "One-dimensional three-state quantum walk," Phys. Rev. E **72**, 056112 (2005).

[45] P. Ribeiro, P. Milman, and R. Mosseri, "Aperiodic Quantum Random Walks," Phys. Rev. Lett. **93**, 190503 (2004).

[46] D. Shapira, O. Biham, A. J. Bracken and M. Hackett, "One-dimensional quantum walk with unitary noise," Phys. Rev. A **68**, 062315 (2003).

[47] A. Schreiber, K.N. Cassemiro, V. Potoček, A. Gábris, I. Jex, and Ch. Silberhorn, "Decoherence and Disorder in Quantum Walks: From Ballistic Spread to Localization," Phys. Rev. Lett. **106**, 180403 (2011).

[48] J. M. Edge and J. K. Asboth, "Localization, delocalization, and topological transitions in disordered two-dimensional quantum walks," Phys. Rev. A **91** , 104202 (2015).

[49] D. Shapira, S. Mozes, and O. Biham, "Effect of unitary noise on Grover's quantum search algorithm ," Phys. Rev. A **67**, 042301 (2003).

[50] D. Hocker, C. Brif, M. D. Grace, A. Donovan, T. S. Ho, K. Moore Tibbetts, R. B. Wu, and H. Rabitz, "Characterization of control noise effects in optimal quantum unitary dynamics ," Phys. Rev. A **90**, 062309 (2014).

[51] A. Chenu, M. Beau, J. Cao, and A. del Campo, "Quantum Simulation of Generic Many-Body Open System Dynamics Using Classical Noise," Phys. Rev. Lett. **118**, 140403 (2017).

[52] M. A. C. Rossi, C. Benedetti, M. Borrelli, S. Maniscalco, and M. G. A. Paris, "Continuous-time quantum walks on spatially correlated noisy lattices," Phys. Rev. A **96**, 040301(R) (2020).

[53] B. Wang, T. Chen, and X. Zhang, "Experimental Observation of Topologically Protected Bound States with Vanishing Chern Numbers in a Two-Dimensional Quantum Walk ," Phys. Rev. Lett. **121**, 100501 (2018).

[54] C. V. C. Mendes, G. M. A. Almeida, M. L. Lyra, and F. A. B. F. de Moura, "Localization-delocalization transition in discrete-time quantum walks with long-range correlated disorder," Phys. Rev. E **99**, 022117 (2019).

[55] E.A. Novikov, "Functions and the random-force method in turbulence theory," JETP **20**, 1290 (1965).

[56] T. Chen, X. Zhang, and X. Zhang, "Quantum sensing of noises in one and two dimensional quantum walks ," Sci. Rep. A **10**, 1038 (2017).

[57] R. Vieira, E. P. M. Amorim, and G. Rigolin, "Entangling power of disordered quantum walks ," Phys. Rev. A **89**, 042307 (2014).

[58] R. Vieira, E. P. M. Amorim, and G. Rigolin, "Dynamically Disordered Quantum Walk as a Maximal Entanglement Generator ," Phys. Rev. Lett. **111**, 180503 (2013).

[59] T. Baumgratz, M. Cramer, and M. B. Plenio, "Quantifying Coherence ," Phys. Rev. Lett. **113**, 140401 (2014).

[60] M. N. Bera, T. Qureshi, M. A. Siddiqui, and A. K. Pati, "Duality of quantum coherence and path distinguish ability ," Phys. Rev. A **92**, 012118 (2015).